Available online at www.sciencedirect.com
SCIENCE DIRECT®
Journal of Photochemistry and Photobiology A: Chemistry 170 (2005) 203–213
Journal of Photochemistry and Photobiology A:Chemistry
www.elsevier.com/locate/jphotochem

Spectral characteristics of methyl 2-aminonicotinate: effect of solvents and acid–base concentrations

Manoj K. Nayak, Sneh K. Dogra*

Department of Chemistry, Indian Institute of Technology Kanpur, Kanpur 208016, India

Received 22 April 2004; received in revised form 23 July 2004; accepted 9 August 2004
Available online 2 October 2004

Abstract

Absorption, fluorescence excitation and fluorescence spectroscopy, combined with time-dependent spectroscopy and semi-empirical AM1 and density functional theory using Gaussian 98 program calculations have been used to study the effect of solvent and acid–base concentration on the spectral characteristics of methyl 2-aminonicotinate (2-MAN). These results have shown that amine–imine equilibrium is absent in 2-MAN, both in the ground (S_0) and first excited singlet (S_1) states. Normal small Stokes shifted emission observed in all the solvents suggest the absence of excited state intramolecular proton transfer (ESIPT) in 2-MAN. Ionic species in S_0 and S_1 states formed at different acid–base concentrations are: Trication (TC), dication (DC1), monocation (MC1) and monoanion (MA), pK_a values for different prototropic equilibrium were determined in S_0 and S_1 states and discussed.

Keywords: Methyl 2-aminonicotinate (2-MAN); Absorption spectrum; Fluorescence spectrum; Prototropic equilibria; Excited state intramolecular proton transfer

1. Introduction

Spectral characteristics of 2-aminopyridine (2-AP) [1–9] and 2-aminobenzoic acid (2ABA) [10–13] have been studied extensively. Besides the basic center of =N-atom in pyridine, 2-AP contains $-NH_2$ group, which can behave like both acidic and basic centers. It is well established [14] that $-NH_2$ group becomes stronger acid and =N-atom becomes stronger base in S_1 state. Thus 2-AP may exhibit amine–imine tautomerism in S_1 state if not in S_0 state. All the studies carried out on 2-AP have shown that 2-AP emits only one small Stokes shifted fluorescence band in all the solvents. This has established that amino-imine tautomerism is absent in this molecule and 2-AP exists only as amine form. The reason could be that the activation barrier for amine to imine conversion is 202.5 kJ mol^{-1} in S_0 state. Although imine form of 2-AP is thermodynamically stable than amino form in S_1 state by 22.17 kJ mol^{-1}, the barrier height for this process is still 173.6 kJ mol^{-1} in S_1 state [6]. Absence of ESIPT in 2-AP could be due to the absence of intramolecular hydrogen bonding (IHB) in S_0 state or due to the smaller acidity of $-NH_2$ group in S_0 and S_1 states.

Even though IHB is present in 2-ABA in S_0 state, ESIPT is not observed in S_1 state. Tramer [11,12] has established that IHB in 2-ABA is between the lone pair of $-NH_2$ and the carboxylic acid proton. In other words 2-ABA is present either in the molecular form or in the zwitterionic form where ESIPT is not possible.

Present work involves the study of spectral characteristics of 2-MAN in different solvents and at different acid–base concentrations. In this molecule, carboxylic acid proton has been replaced by a methyl group. Thus there can be only one kind of IHB between the amino proton and the carbonyl oxygen lone pair, which can lead to ESIPT. This molecule can be considered as a composite of two systems; one as 2-AP and the second methyl 2-aminobenzoate (2-MAB). The present study has been carried out with the following aims in mind. (i) Electron withdrawing carboxylic acid group present at *ortho* position to amino group will increase the acidity of amino group both in S_0 and S_1 states. The existence of amine-imino phototautomerism may thus be possible. (ii) One of

* Corresponding author. Tel.: +91 512 597 163; fax: +91 512 5974 36.
E-mail address: skdogra@iitk.ac.in (S.K. Dogra).

1010-6030/$ – see front matter © 2004 Elsevier B.V. All rights reserved.
doi:10.1016/j.jphotochem.2004.08.013

the criteria of ESIPT is that the acidity and basicity of the proton donor and proton acceptor groups must increase in S_1 state. Although the pK_a values for the deprotonation of $-NH_2$ group decreases from >16 in S_0 state to ∼11 in the S_1 state [15–20], this may not be large enough for ESIPT. Presence of electron withdrawing =N-atom at the *ortho* to $-NH_2$ group can increase the acidity of $-NH_2$ group both in S_0 and S_1 states and can increase the feasibility of ESIPT. Besides these points in mind, effect of acid–base concentration has been studied on the spectral characteristics. Dissociation constants for the various prototropic equilibria have been determined both in S_0 and S_1 states and discussed. AM1 semi-empirical quantum mechanical and DFT and TD (DFT) B3LYP with 6-31G** basis set calculations have also been carried out to assign the spectral characteristics to various species involved in the system.

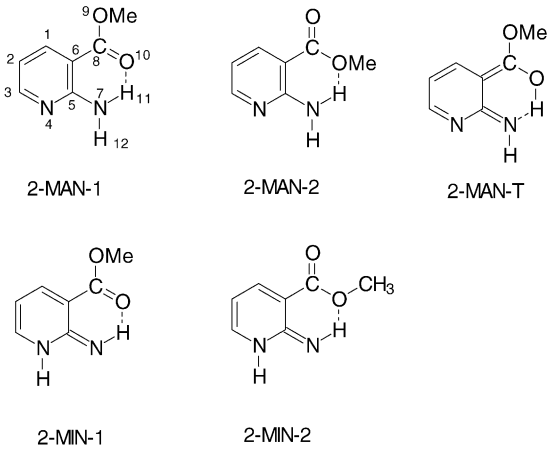

Scheme 1.

2. Materials and methods

2-Aminonicotinic acid (2-ANA) was obtained from Aldrich Chemical Company (U.K.) and methyl ester (2-MAN) was prepared by refluxing 2-ANA in methanol containing more than three equivalents of H_2SO_4, as described in literature [21]. 2-MAN was purified by repeated crystallization from methanol. Purity of the compound was checked by single spot on TLC, NMR and getting similar fluorescence excitation spectra when monitored at different emission wavelengths (λ_{em}). All the solvents used were either of spectroscopic grade or HPLC grade from E. Merck and were used as received. Spurious emission was checked for each solvent by exciting at the same wavelength as used for each solution of 2-MAN in different solvents. Triply distilled water was used for the preparation of aqueous solutions.

Procedure used to prepare solutions and adjustment of pH was the same as described in our recent papers [22,23]. Since 2-MAN is sparingly soluble, saturated solution of 2-MAN was prepared in all the solvents and then diluted according to have the desired absorbance. Hammett's acidity scale [24] was used for H_2SO_4/H_2O mixtures for pH < 1 and Yagil's basicity scale [25] was used for NaOH/H_2O mixtures for pH > 13. Details of the instruments used for recording absorption, fluorescence excitation and fluorescence spectra, measuring lifetimes in the excited states and pH are the same as described in our recent papers [22,23]. Fluorescence quantum yield (Φ_f) was measured from solutions having absorbance less than 0.1 using quinine sulphate in 1N H_2SO_4 as reference [26] (Φ_f = 0.55).

3. Semi-empirical calculations

Scheme 1 represents various amino rotamers, (2-MAN-1, 2-MAN-2), tautomer (2-MAN-T) and imino rotamers (2-MIN-1, 2-MIN-2). AM1 semi-impirical quantum mechanical calculations [27] (QCMP 137, MOPAC 6/PC) were carried out to get various parameters for the fully optimized geometries of all the species in S_0 state. This method provides acceptable approximations to give results which are quite close to the experimental results, as observed by others [28–31]. Total energy relative to the most stable species (E), dipole moment (μ) and charge densities at different basic centers are compiled in Table 1. Transition energies (ΔE_{ij}) have been calculated using CNDO/S-CI method, as suggested by Del Bene and Jaffe [32] and described in our recent publications [22,23]. Long wavelength (LW) transition for each species is complied in Table 2. Charge densities in S_1 state at different basic centers have been obtained by CNDO/S-CI method [33] and are compiled in Table 1. Transition energies (ΔE_{ij}) were also calculated using standard single point calculations AM1 method and are compiled in Table 2. Geometry of each species was also optimized using AM1 method and taking into account the configurational interactions (CI = 5 in MOPAC, 100 configurations). Emission transitions were obtained by using the single point calculations and considering the geometry of the species in S_1 state. Desired transition energies obtained by this method along with experimental data are compiled in Table 2.

Dipolar solvation energies for different states were calculated using the following expression based on Onsager's theory [34]

$$\Delta E_{sol} = -\left(\frac{\mu^2}{a^3}\right) f(D) \quad (1)$$

where $f(D) = (D-1)/(2D+1)$, D is dielectric constant of the solvent, μ dipole moment in the respective state and 'a' Onsager's cavity radius. For non-spherical molecules, value of 'a' has been calculated by taking 40% of the maximum length of the molecule [35] and the value is 0.317 nm. Total energies including solvation energies for each species in water are also given in Table 1. It may be mentioned here that we have not taken into account the specific interactions, like hydrogen bonding etc. for calculating the total energies.

Table 1
Calculated parameters of 2-MAN rotamers/tautomers in the ground and excited states

Parameters	2-MAN-1	2-MAN-2	2-MAN-T	2-MIN-1	2-MIN-2
S_0 state					
AM1 method					
ΔH_f (kcal mol^{-1})	−53.5	−51.3	−21.7	−34.6	−33.2
E (kJ mol^{-1})	0	9.4	133.0	79.0	85.0
E_{sol} (kJ mol^{-1})	0	7.2	125.0	63.0	77.1
$\mu_{g\,(D)}$	1.0	1.9	3.2	4.3	2.9
DFT method					
E (kJ mol^{-1})	0	12.2	–	75.1	119.7
$\mu_{g\,(D)}$	1.14	2.1	–	4.5	5.0
S_1 state					
AM1 method					
ΔH_f (kcal mol^{-1})	21.2	25.8	46.9	26.7	28.1
E (kJ mol^{-1})	0	19.3	107.4	22.4	28.8
E_{sol} (kJ mol^{-1})	10.1	20.9	87.6	0	17.3
Charge densities					
CNDO/S-CI method					
S_0					
N_4	−0.311	−0.306	−0.310		
N_7	−0.271	−0.272	−0.427		
O_9	−0.254	−0.252	−0.251		
O_{10}	−0.473	−0.467	−0.267		
S_1					
N_4	−0.143	−0.16	−0.266		
N_7	−0.259	−0.254	−0.232		
O_9	−0.244	−0.230	−0.248		
O_{10}	−0.263	−0.259	−0.275		

Three possible monocations (MCs) and three possible dications (DCs), Scheme 2, were also considered. AM1 semi-empirical quantum mechanical calculations were also performed on these species and the relevant data are compiled in Tables 3 and 4 respectively. Dipolar solvation energies in water were calculated in water as solvent using Eq. (1).

The electronic structure calculations were also performed on each species, as mentioned in Schemes 1 and 2, using Gaussian 98 program [36]. The geometry optimization was performed on each species of 2-MAN in S_0 state using DFT [37,38] B3LYP with 6-31G** basis set [36,39]. The geometry of these stationary points on S_1 state was calculated using

Table 2
Assignment of the excitation and fluorescence transitions of 2-MAN in terms of calculated energies (eV) with and without solvation and experimental values

Assignment	2-MAN-1	2-MAN-2	2-MAN-T	2-MIN-1	2-MIN-2
Excitation					
Without solvation					
Single point	3.332	3.390	3.096	2.908	2.957
CNDO/S-CI	4.034	4.120	3.523	3.613	3.669
TD (DFT)	4.00	4.094	–	3.172	3.445
Experimental	3.76				
With solvation					
Single point	3.338	3.363	3.136	2.982	2.972
Experimental	3.76				
Emission					
Without solvation					
Single point	3.133	3.193	2.399	2.335	2.287
Experimental	3.381				
With solvation					
Single point	3.136	3.133	2.251	2.254	2.197
Experimental	3.158				

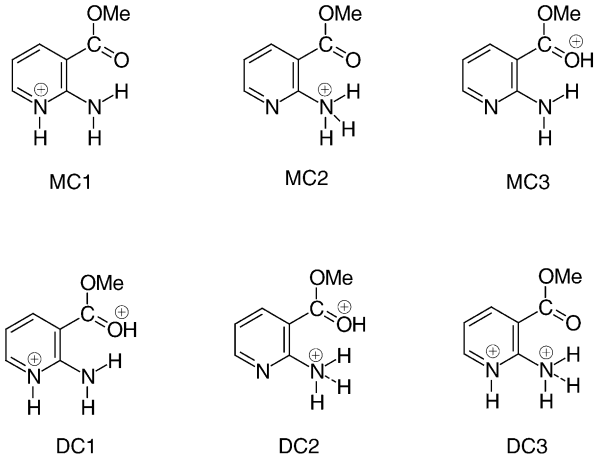

Scheme 2.

configuration interaction singles (CIS) [37,40] theory with 6-31G** basis sets. Time-dependent (TD) [41,42] DFT B3LYP was also used to calculate stationary point geometry in S_0 and S_1 states. Relevant data are compiled in Tables 1–4.

Table 3
Calculated parameters of the monocations of 2-MAN in the ground and excited states

Parameters	MC1	MC2	MC3
S_0 state			
AM1 method			
ΔH_f (kcal mol^{-1})	95.8	106.3	113.4
E (kJ mol^{-1})	0.0	43.8	73.7
E_{sol} (kJ mol^{-1})	0.0	76.9	117.7
$\mu_{g(D)}$	7.5	4.6	3.1
$\Phi(N_7C_5N_4C_3)$ (deg)	−180	−180	−179
DFT method			
E (kJ mol^{-1})	0.0	57.2	88.8
$\mu_{g(D)}$	6.8	3.7	3.1
S_1 state			
AM1 method			
ΔH_f (kcal mol^{-1})	180.2	206.4	175.7
E (kJ mol^{-1})	41.3	128.7	0.0
E_{sol} (kJ mol^{-1})	0.0	149.8	31.1
$\mu_{e(D)}$	9.0	3.7	1.7
Transition energies (nm)			
Absorption			
Single point			
S_0–S_1	357	262	422
CNDO/S-CI			
S_0–S_1	343 (n, π*)	309 (n, π*)	318 (π, π*)
S_0–S_2	295 (π, π*)	267 (n, π*)	279 (n, π*)
TD (DFT)			
S_0–S_1	290 (π, π*)	258 (n, π*)	329 (n, π*)
S_0–S_2	284 (n, π*)	255 (n, π*)	288 (π, π*)
Emission			
Single point			
S_1–S_0	341	362	609

Table 4
Calculated parameters of the dications of 2-MAN in the ground and excited states

Parameters	DC1	DC2	DC3
S_0 state			
AM1 method			
ΔH_f (kcal mol^{-1})	350.8	363.7	365.5
E (kJ mol^{-1})	0.0	54.0	61.3
E_{sol} (kJ mol^{-1})	53.1	115.9	0.0
$\mu_{g(D)}$	4.3	3.0	11.9
DFT method			
E (kJ mol^{-1})	0.0	71.2	25.5
$\mu_{g(D)}$	4.4	5.9	10.6
S_1 state			
AM1 method			
ΔH_f (kcal mol^{-1})	434.7	442.7	429.4
E (kJ mol^{-1})	18.6	51.1	0.0
E_{sol} (kJ mol^{-1})	16.4	51.9	0.0
$\mu_{e(D)}$	5.5	5.2	5.2
Transition energies (nm)			
Absorption			
Single point			
S_0–S_1	335	336	299
CNDO/S-CI			
S_0–S_1	291 (π, π*)	291 (n, π*)	362 (n, π*)
S_0–S_2	275 (π, π*)	276 (π, π*)	265 (π, π*)
TD (DFT)			
S_0–S_1	243 (n, π*)	330 (n, π*)	285 (n, π*)
S_0–S_2	241 (π, π*)	286 (π, π*)	284 (n, π*)
Emission			
Single point			
S_1–S_0	368	438	792

4. Results

4.1. Effect of solvents

Absorption spectrum of 2-MAN have been recorded in different solvents. The relevant data are compiled in Table 5. Molecular extinction coefficients could not be calculated accurately except in water because of poor solubility in each solvent. LW absorption band is a doublet, with vibrational frequency 890 cm^{-1} and the structure is retained even in the most polar solvent water. Both the absorption band maxima (λ^{ab}_{max}) are unaffected with increase in polarity and hydrogen bonding capacity of the solvents. Full width at half the maximum height (FWHM) increases under the above environments. λ^{ab}_{max} of 2-MAN in any solvent are red shifted in comparison to 2-AP [1], methyl nicotinate (MN) [43] and methyl 6-aminonicotinate (6-MAN) [44] but are nearly similar to 2-ABA [13].

4.2. Fluorescence spectrum

Fluorescence spectrum of 2-MAN in some selected solvents are shown in Fig. 1 and the relevant data are compiled in

Table 5
Absorption band maximum (λ^{ab}_{max}, nm), fluorescence band maximum (λ^{f}_{max}, nm), fluorescence quantum yield (Φ_f), lifetime in S_1 state (τ, ns), radiative (k_r, $10^7\ s^{-1}$) and non-radiative (k_{nr}, $10^7\ s^{-1}$) rate constant of 2-MAN in different solvents

Solvent	λ^{ab}_{max}			λ^{f}_{max} Φ_f	τ	k_r	k_{nr}
Cyclohexane	247	329	340	367 (0.487)	5.47	8.9	9.38
Ether	248	332	340	379 (0.57)	6.24	9.13	6.89
Dioxane	250	330	340	381 (0.60)	7.23	8.30	5.53
Ethyl acetate	255	332	340	381 (0.51)	5.70	8.94	8.81
Acetonitrile	247	330	340	381 (0.535)	6.44	8.30	7.23
n-Propanol	250	330	340	386 (0.615)	7.04	8.73	5.47
Methanol	247	331	340	387 (0.622)	6.84	9.09	5.53
Water pH 6.8	248	326	–	393 (0.72)	9.03	7.97	3.10
Water pH 2.0	243	328	–	387 (0.008)	0.6	1.33	165.3
Water $H_0 = -5.05$	247	327	–	384 (0.736)	8.54	8.62	3.09
Water $H_0 = -10.05$	243	326	–	402 (0.73)	7.03	10.38	3.84
Water $H_- = 16$	243	316	–	501 (0.0065)	0.24	2.7	414.0

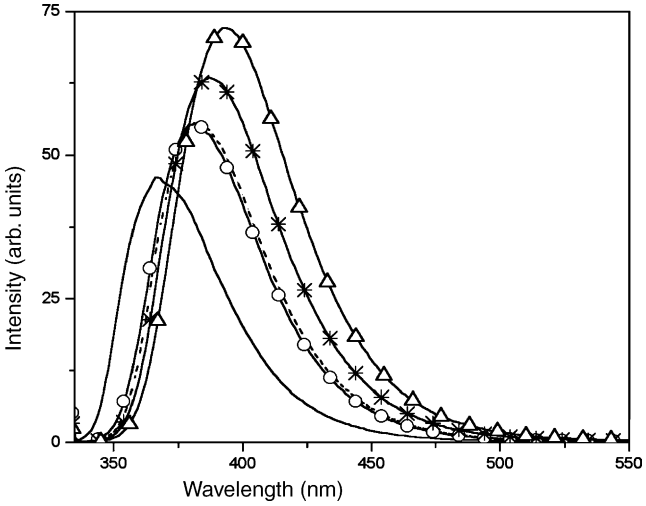

Fig. 1. Fluorescence spectrum of 2-MAN in some selected solvents. (—), cyclohexane; (- - -), dioxane; (◯—◯—◯), acetonitrile; (✳), methanol; (Δ—Δ—Δ), water pH 6.8. At λ_{exc} = 330 nm.

Table 5. Unlike absorption spectrum, fluorescence spectrum is relatively more sensitive to solvent characteristics, indicating that 2-MAN is more polar in S_1 state than in S_0 state. A continuous red shift is observed in the fluorescence band maxima (λ^{f}_{max}) of 2-MAN with increase in solvent polarity and hydrogen bonding nature. This suggests a better delocalization of π-cloud of carbonyl group and the lone pair of amino group with the pyridine ring. Under the similar environments, FWHM of the fluorescence band does not change but Φ_f increases in going from cyclohexane to water. FWHM of the fluorescence band in each solvent is smaller than that of the LW absorption or fluorescence excitation band (see latter). It may be concluded that 2-MAN is less flexible in S_1 state in comparison to that in S_0 state. Although there is no change in the planarity of the substituents with the pyridine ring, the bond distances r (C_5–N_7) and r (C_6–C_8) reduces to 0.135 nm and 0.143 nm in S_1 state from 0.138 nm and 0.146 nm in S_0 state, respectively. Normal Stokes shifted fluorescence band observed in each solvent suggests that ESIPT does not occur in S_1 state. This behavior is similar to 2-ABA [11,12] but different from 2-amino-3-naphthoic acid [45]. λ^{f}_{max} of 2-MAN is red shifted in comparison to 2-AP [1] but occur nearly at the same region as observed in 2-ABA [11,12].

4.3. Fluorescence excitation spectrum

Fluorescence excitation spectra of 2-MAN were also recorded in different solvents and at different emission wavelengths (λ_{em}) in the range of 350–420 nm. In each solvent and in each case fluorescence excitation spectrum recorded at different λ_{em} resemble with each other and also with absorption spectrum in all aspects (i.e. λ^{ab}_{max} and FWHM). Overlap of the fluorescence band with fluorescence excitation spectrum in each solvent suggests that emission is a normal Stokes shifted one. This indicates that there is only one species in S_0 state. Overlap between fluorescence excitation and fluorescence spectrum is maximum in cyclohexane and the overlap decreases with increase in the polarity and hydrogen bonding nature of the solvents. This is due to the shift of fluorescence spectrum towards red of absorption spectrum in polar solvents, suggesting that the molecule is more polar in S_1 state and larger solvent relaxation is occurring in polar solvents, rather than due to larger changes in geometry of the molecule in S_1 state in comparison to S_0 state. This is also supported by the data of Table 1.

4.4. Excited state dipole moment

Excited state dipole moment (μ_e) can be evaluated by using number of equations and spectral data. We have used only Bilot-Kawski's (BK) Eq. (2) [46] in this work.

$$\bar{\nu}_{ab} - \bar{\nu}_{fl} = m\left[\frac{D-1}{2D+1} - \frac{n^2-1}{2n^2+1}\right] \quad (2)$$

$$m = \frac{(\mu_e - \mu_g)^2}{\beta a^3} \quad (3)$$

and $\beta = 2\pi\varepsilon_o hc = 1.105 \times 10^{-35}\ C^2$, h Planck's constant, c velocity of light, $4\pi\varepsilon_0$ is the permittivity constant, $\bar{\nu}_{ab}$ and $\bar{\nu}_{fl}$ are the absorption and fluorescence band maxima in

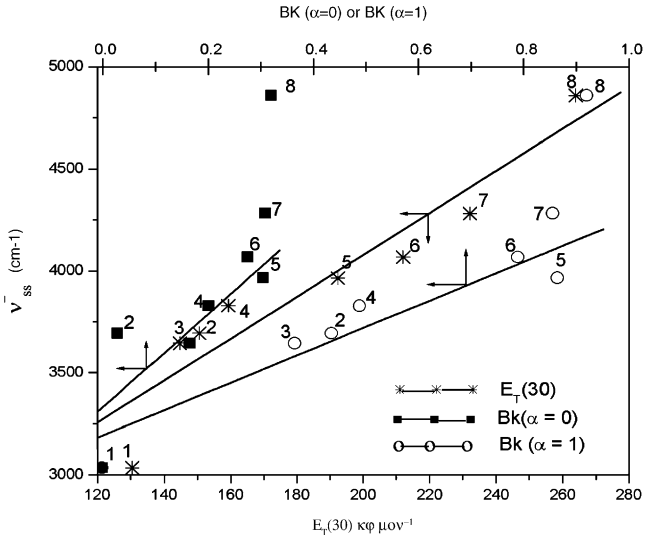

Fig. 2. Plot of Stokes shifts versus different polarity parameters. (✳), $E_T(30)$; (■—■—■), BK parameters, $\alpha = 0$; (○—○—○), $\alpha = 1$.

wave numbers (cm^{-1}). In case of isotropic polarizability (α = polarizability) of molecules, condition $2\alpha/4\pi\varepsilon_o a^3 = 1$, is frequently satisfied and Eq. (2) will represent BK equation. When $\alpha = 0$, (polarizability is neglected), Eq. (2) is reduced to Eq. (4), derived by Lippert [47] and Mataga [48].

$$\bar{\nu}_{ab} - \bar{\nu}_{fl} = m\left[\frac{D-1}{2D+1} - \frac{n^2-1}{2n^2+1}\right] \quad (4)$$

BK polarity parameters for $\alpha = 0$ and $\alpha = 1$ were taken from literature [49] and value of $\bar{\nu}_{ab}$ in each solvent is taken from the fluorescence excitation spectrum as it is more sensitive. Fig. 2 represents the plot of Stokes shifts ($\bar{\nu}_{ss}$) versus polarity parameters when $\alpha = 0$ and $\alpha = 1$. $\bar{\nu}_{ss}$ versus $E_T(30)$ polarity parameter is also depicted in Fig. 2. Except $E_T(30)$ plot, departure from linear relations (Eqs. (4) and (2)) is quite large for protic solvents as observed in other aromatic amines [15–20] and thus can be explained in the same manner. On the other hand $E_T(30)$ parameters takes care of the specific interactions. Change in dipole moment $\Delta\mu = \mu_e - \mu_g$ was calculated from the linear part of the plots after neglecting dioxane and protic solvents and using 'a' as 0.317 nm. Values are found to be 2.69 *D* and 1.85 *D* for $\alpha = 0$ and $\alpha = 1$ respectively. Peculiar properties of dioxane are well known and the large deviations from the linearity observed in this solvent can be explained on the same lines as made by Ledger and Suppan [50].

4.5. Excited state lifetimes

Lifetime (τ) of 2-MAN in different solvents were measured by using λ_{exc} = 337 nm and λ_{em} as the fluorescence band maximum in each solvent. Fluorescence intensity profile in each case followed a single exponential decay $\chi^2 = 1 \pm 0.1$ and good autocorrelation function. It is observed that τ is independent of λ_{exc} and λ_{em}. Fig. 3 represents a

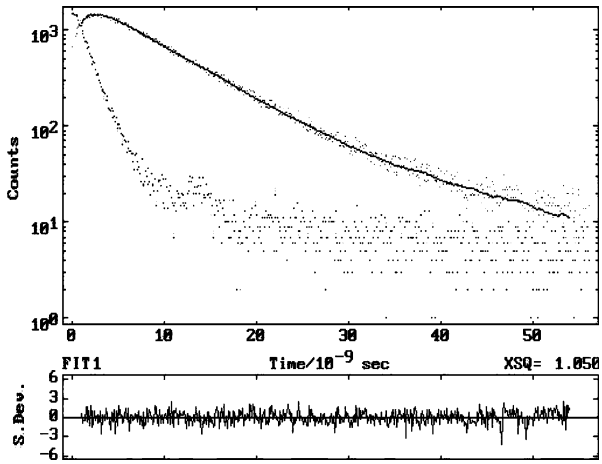

Fig. 3. Fluorescence decay profile of 2-MAN in methanol. λ_{exc} = 337 nm, λ_{em} = 386 nm.

typical fluorescence decay profile of 2-MAN in methanol as solvent. Values of radiative (k_r) and non-radiative (k_{nr}) rate constants were calculated from the lifetimes (τ) and Φ_f using the following relations. Values of τ, Φ_f, k_r and k_{nr} in different solvents and at different acid–base concentrations are compiled in Table 5. Values of k_r in different solvents are nearly independent of the characteristics of solvents, whereas those

$$k_r = \frac{\Phi_f}{\tau}, \quad k_{nr} = \frac{1}{\tau - k_r}$$

of k_{nr} decreases with increase of solvent polarity and hydrogen bond forming capacity of the solvents. Values of k_{nr} for the monocation (MC) and monoanion (MA) are very large (1.65×10^9 and $4.14 \times 10^9\ s^{-1}$, respectively) as compared to other ionic species.

4.6. Effect of acid–base concentrations

Absorption and fluorescence spectra of 2-MAN were investigated in the acid–base concentration range of H_0/pH/H_- −10.0–16. Relevant data are compiled in Table 5 and respective spectra are shown in Figs. 4 and 5, respectively. 2-MAN is neutral in the pH range of 6.8 to 10 in S_0 state. With increase of base strength a blue shifted absorption band appears at 316 nm having an isosbestic point at 314 nm. No change is observed in the absorption spectrum at $H_- > 15$. 316 nm band can be assigned to monoanion (MA) formed by the deprotonation of $-NH_2$ group. With decrease of pH λ^{ab}_{max} at 326 nm is shifted to 328 nm, whereas 248 nm band to 243 nm. There is an increase in the absorbance at 328 nm by 30% with an isosbestic point at 340 nm. These changes could be assigned to the formation of monocation (MC) at pH ∼ 2.0. With further increase of acid strength hardly any change is observed in λ^{ab}_{max} even up to $H_0 = -10.0$. So nothing can be said about further protonation of MC from absorption data. pK_a values of MC-N and N-MA equilibria have been calculated from absorption data and are given on the arrows

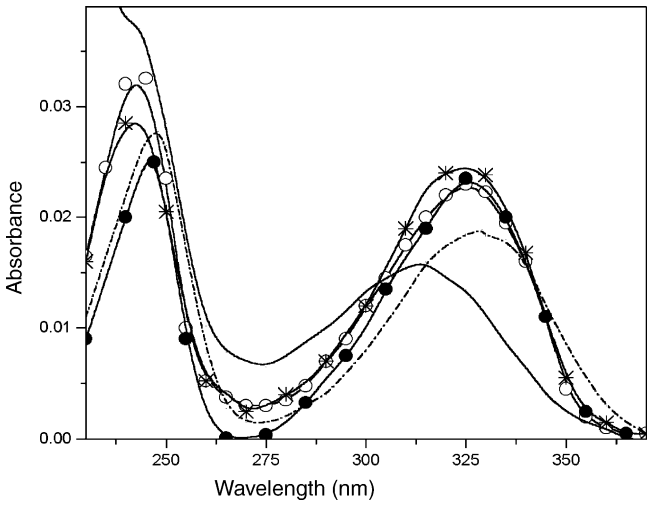

Fig. 4. Absorption spectrum of different ionic species. (—), H_- = 16; (- - -), pH 6.80; (◯—◯—◯), pH 2.0; (●—●—●), H_0 = −5.0; (✳), H_0 = −10.05. [2-MAN] = 2×10^{-6} M.

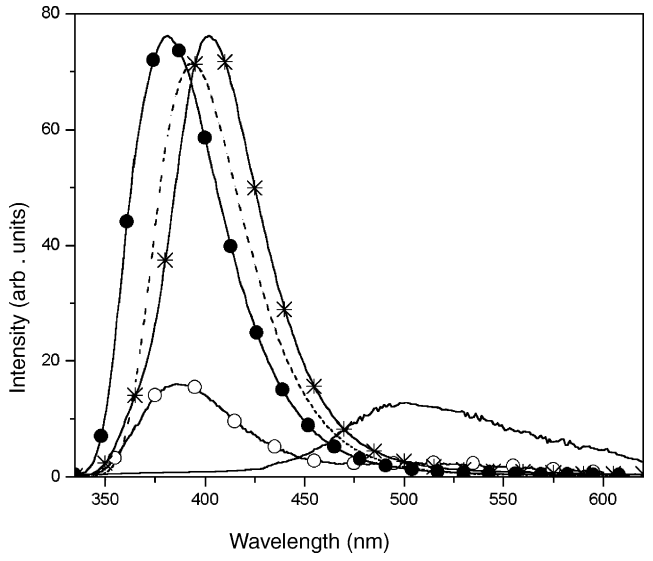

Fig. 5. Fluorescence spectrum of different ionic species. (—), H_- = 16 (intensity enhanced 40 times); (- - -), pH = 6.80; (◯—◯—◯), pH 2.0 (intensity enhanced 20 times); (●—●—●), H_0 = −5.0; (✳), H_0 = −10.05. At λ_{exc} = 325 nm and [2-MAN] = 2×10^{-6} M.

of the respective equilibria (Scheme 3). Unlike absorption spectrum, a very weak and large red shifted fluorescence band (501 nm) appears with increase of base concentration. This fluorescence band is very similar to that observed in case of 2-naphthylamine [19] under the similar NaOH concentration and thus can be assigned to MA formed by the deprotonation of $-NH_2$ group. With decrease of pH fluorescence intensity of neutral 2-MAN (393 nm) is quenched with the appearance of small blue shifted weak emission (387 nm) and remains unchanged up to H_0 = 0. With further increase of acid strength, fluorescence intensity increases with the appearance of an emission band at 384, reaches a maximum value at H_0 = −5.0. At H_0 < −5.0 a new intense red shifted emission band appears at 402 nm with an isoemissive point at 393 nm.

pK_a values in S_1 state (pK_a^*) were calculated using fluorimetric titration curves. Due to poor fluorescence intensities of some of the ionic species, the fluorescence intensities of either conjugate acid or conjugate base were plotted. Values obtained are given below the arrows of Scheme 3. Fluorescence decay profiles of each ionic species followed single exponential and lifetime obtained are compiled in Table 5. This suggests that only one kind of ionic species is present at the respective acid–base concentrations. Lifetime of the species at pH 2 could not be measured because of very small fluorescence intensity.

4.7. Effect of acid–base concentration in non-aqueous solvents

Spectral characteristics of 2-MAN were also studied in acetonitrile and methanol containing different concentrations of H_2SO_4 up to 1 M. Absorption characteristics of 2-MAN in acidified acetonitrile and methanol are similar to those observed in water i.e. small blue shifted band appears at 325 nm in acetonitrile and 328 nm in methanol. Unlike in aqueous medium, fluorescence band of neutral 2-MAN is not quenched with increase of acid concentration, but slightly more intense and a red shifted emission band appears at 384 nm and 1×10^{-3} M H_2SO_4, followed by a slightly blue shifted band at 381 nm at 1 M H_2SO_4.This behaviour is similar to those observed in water at pH 2 and H_0 = −5 respectively. Fluorescence excitation spectra recorded at 1×10^{-2} M and 1 M H_2SO_4 at different λ_{em} in acetonitrile were similar to each other and resemble with the absorption spectrum, suggesting that the absorbing and emitting species are the same at these two respective acid concentrations. Intersection of fluorescence excitation and fluorescence spectra suggests the presence of small Stokes shifted fluorescence band. Excited state lifetimes of 2-MAN in an acetonitrile containing 1×10^{-2} M and 1 M H_2SO_4 and using λ_{exc} = 337 nm and λ_{em} 384, 460 are similar to each other (9.0 ± 0.1 ns). This indicates the presence of only one kind of MC.

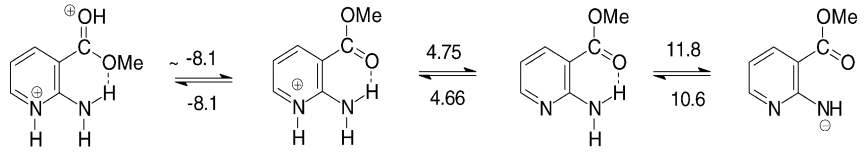

Scheme 3.

5. Discussion

5.1. Assignment of states

Before we start the discussion, it may be mentioned here, unlike 2-ABA, there can be only one kind of IHB in 2-MAN, i.e. between the carbonyl oxygen atom or $-OCH_3$ and amino proton (2-MAN-1 and 2-MAN-2). From Table 1, it is clear that both the rotamers (2-MIN-1 and 2-MIN-2) are less stable than 2-MAN-1 by 79 and 85 kJ mol^{-1} under isolated conditions in S_0 state. The stability of these species will increase on including the solvation energies as μ of the imine forms are greater than that of 2-MAN-1 but the instability is still quite large that imine forms can be neglected in S_0 state in any solvent. Results based on heats of formation and DFT calculations also suggest that 2-MAN-1 is the most stable species. The conclusion is supported by the fact that activation barrier for this IPT in S_0 state is 401 kJ mol^{-1}. Very large value of activation barrier for this IPT could be due the formation of four memebred ring conformation between hydrogen donor ($-NH_2$ group) and hydrogen acceptor (=N-atom) in 2-MAN so that IPT reaction is expected to be associated with very large strain energy. In S_1 state 2-MAN-1 is still the most stable species under isolated conditions, whereas 2-MIN-1 becomes the most stable species when dipolar solvation energy is included. This species still can be neglected on the grounds that the activation barrier for IPT is very large (336 kJ mol^{-1}). Similar behavior is also observed in 2-AP [6]. In other words, it may be concluded that 2-MAN-1 will be present as amino form both in S_0 and S_1 states.

Similarly the presence of tautomer (2-MAN-T) form can also be neglected in S_0 state in any solvent because the proton transfer from $-NH_2$ group to >C=O group is endothermic by 133 kJ mol^{-1} under isolated conditions and by 125 kJ mol^{-1}when dipolar solvation energy is included. Further the activation barrier height for the conversion of 2-MAN-1 to 2-MAN-T is 151 kJ mol^{-1} and thus makes this process unviable at room temperature. In case of DFT, the optimized structure of 2-MAN in S_0 state is always 2-MAN-1 even if we start with 2-MAN-T. Combining the results of heats of formation along with DFT results, presence of 2-MAN-T can also neglected in S_0 state. Although the stability of 2-MAN-T increases in S_1 state (Table 1, 107.4 kJ mol^{-1}) and the activation barrier also decreases from 151 to 121.5 kJ mol^{-1}, these values are still quite large to conclude that 2-MAN-T will be absent in S_1 state also.

Rotamer 2-MAN-2 is unstable by 9.4 kJ mol^{-1} under isolated conditions and 7.2 kJ mol^{-1} when dipolar solvation is added. Activation energy for the conversion of 2-MAN-1 to 2-MAN-2 in S_0 state is 22.7 kJ mol^{-1} under isolated conditions and will decrease when dipolar solvation energy is added. Thus presence of 2-MAN-2, even though in small amounts, cannot be ruled out in the system. This can be supported by the data of Table 2 that the predicted absorption transitions for the rotamers 2-MAN-1 and 2-MAN-2 are quite close to the experimentally observed ones. The agreement between the results predicted by all the methods is quite close to the experimental results. In S_1 state, conversion of 2-MAN-1 to 2-MAN-2 will be further hindered because the stability of 2-MAN-1 increases from 9.4 to 19.3 kJ mol^{-1} under isolated conditions and from 7.2 to 10.8 kJ mol^{-1} when dipolar solvation energy is included. The activation barrier for this conversion in S_1 state also increases from 22.7 to 45.6 kJ mol^{-1}. This seems to be consistent with the fact that carbonyl oxygen becomes stronger base and thus will increase the hydrogen bond strength.

CNDO/S-CI calculations have predicted that S_1 and S_2 states of 2-MAN are of n, π^* and π, π^* in nature, respectively. This is in agreement with those predicted for 2-AP [1] and by Jain et al. for 2-ABA respectively [13]. Large value of molecular extinction coefficient and very high value of Φ_f suggest that the lowest energy absorption band observed can be assigned to S_0–S_2 transition and the next one to S_0–S_3 transition. Similar conclusions have also been arrived at by Jain et al. [13]. On the other hand, Goodman and Shull [51] have explained the near ultra violet absorption band of 2-ABA as being due to intramolecular charge transfer transition from aniline residue to the antibonding orbital of >C=O group. On the other hand, TD (DFT) calculations suggested π, π^* and n, π^* to be S_1 and S_2 states. Gap between S_1 and S_2 states predicted by CNDO/S-CI and TD (DFT) is only 2180 and 4510 cm^{-1}, respectively. A similar behaviour is observed in case of 1-hydroxy-9-fluorenone [52]. It may thus be concluded that if n, $\pi^*$and π, π^* states are close by, prediction and assignment of electronic states by these theories is a difficult proposition. Spectral characteristics in the present case can be explained by mixing the two states. Decrease in k_{nr} with increase in solvent polarity supports this, i.e. increase in solvent polarity decreases the energy of $\pi\,\pi^*$ state and increases that of n π^* state. This will increase the characteristics of $\pi\,\pi^*$ state in the lowest energy transition and increase Φ_f.

It is well known that electron migration or charge transfer interaction between the substituent and the aromatic hydrocarbon is the most important factor which affects and determines the electronic spectra of aromatic hydrocarbon derivatives [53]. The effect of solvents on the spectral characteristics of 2-MAN by these interactions can be obtained by comparing the absorption spectrum of 2-MAN, with 2-AP [1], methyl nicotinate [43] and 2-ABA [13]. Red shift observed in the LW absorption band of 2-MAN as compared to first two molecules and near resemblance with that of 2-ABA, suggests that IHB plays a major role in affecting the near ultraviolet absorption band of 2-MAN. This is supported by the fact that IHB is quite strong in the S_0 and S_1 states, i. e. 22.7 and 45.4 kJ mol^{-1} in 2-MAN-1 and 13.3 and 26.1 kJ mol^{-1}, respectively in 2-MAN-2. Near invariance of the absorption spectra of 2-MAN in different solvents could be due to the accidental cancellation of the effects of intermolecular hydrogen bonding of the solvents with =N– and carbonyl group and NH_2 group. Former leads to red shift and latter to blue shift in the absorption spectrum.

Small Stokes shift observed in different solvents for 2-MAN can be explained as follows. As mentioned above, there is an IHB between the amino proton and the lone pair of carbonyl oxygen atom. It is shown that electronic delocalization is possible through the hydrogen bond. In the excited singlet state this delocalization would be stronger than that in S_0 state, because the electronic orbital is more extended, the ionization potential of the carbonyl group becomes smaller, and the electron affinity of the amine group becomes larger in the excited electronic state than in S_0 state. But due to closer proximity of these two groups, charge separation between the two groups will be small and thus may results in smaller Stokes shift. This may be the main reason for the small slope observed in the Fig. 2 for both α = 0 and α = 1. Lastly, increase in Φ_f with increase in polarity and hydrogen bonding nature of the solvents is due to the competition between inter and intra molecular hydrogen bonding (IHB). It has been established [54] that IHB plays the major role in the non-radiative decay rate constant as compared to intermolecular hydrogen boding. Thus decrease in k_{nr} in going from cyclohexane to water could be due to the partial replacement of IHB by intermolecular hydrogen bonding.

5.2. Monocation-neutral equilibrium

Three MCs can be obtained by protonating three basic centers of 2-MAN. ΔH_f, AM1 and DFT calculations have shown that MC1 is the most stable MC in S_0 state, both under isolated and solvated conditions. On the other hand in S_1 state MC3 is the most stable under isolated conditions and MC1 when dipolar solvation energy is included. So it seems that MC1 is the only MC present in both the states in aqueous medium. This is supplemented by the following results. (i) pK_a value for the protonation of 2-AP [2] at =N-atom is 6.75 and that of >C=O group is ~ -5.0 [14]. pK_a values for the MC–N equilibrium of 2-MAN is 4.75. Thus agrees with the formation of MC1. Small decrease in the pK_a value in 2-MAN is due to the fact that $-NH_2$ group lone pair is shared by two electron withdrawing groups and thus charge density will be smaller on =N– in 2-MAN as compared to that in 2-AP. It is well known that >C=O oxygen becomes strong base in S_1 state and the pK_a^* value increases [14]. But such an increase from -5 in S_0 state to 4.7 in S_1 state is not observed in earlier cases [14]. (ii) In general large red shift is observed in the spectral characteristics of neutral species on protonation of >C=O group [14]. In our case slight red shift in absorption band maxima (2 nm) and slight blue shift in emission spectrum contradicts the protonation of >C=O group. (iii) Ground state pK_a value observed from fluorimetric titration only suggests that prototropic equilibrium is not established in S_1 state. This could be due to smaller value of deprotonation/protonation rate constants in comparison to radiative decay rate constants for the conjugate acid–base pair.

5.3. Dication–monocation equilibrium

Similar to MCs, three DCs can be obtained by further protonating the MCs (Scheme 2). Based on the results of AM1, ΔH_f and DFT calculations, DC1 is the most stable species under isolated conditioned in S_0 state, whereas when dipolar solvation energies are added DC3 is the most stable species. In S_1 state, AM1 calculations predict that DC3 is the most stable DC, both under isolated and solvated conditions. Based on absorption spectral data, it is not possible to assign the nature of DC, as hardly any change is observed in λ_{max}^{ab} except that absorbance increases. On the other hand, fluorescence intensity of 387 nm band increases by a factor of $\sim$80, followed by a blue shift of 3 nm. Although based on the theoretical and experimental data, it is not easy to assign the structure of DC, but based on earlier results [1,2,11,12], it is speculated that DC1 is the most probable species and is supported by the following arguments. (i) Two positive charges are well separated and thus repulsive interaction will be the minimum. (ii) Hardly any changes are observed in the absorption spectrum of nicotinic acid [43] and 2-ABA [13] when protonated at carbonyl oxygen. (iii) pK_a values for the protonation of $-NH_2$ group in MC of 2-AP is -7.8 and pK_a^* could not be determined as it required further stronger conditions to protonate $-NH_2$ is S_1 state [12]. Presence of electron withdrawing –COOMe group at *ortho* position will further decrease in the pK_a value it. In case of 2-ABA pK_a value for the similar prototropic reaction is 2.55 [13]. In case of 2-ABA and 2-DMABA a continuous red shift was observed when acid concentration was increased from 0.5 to 10 M H_2SO_4, followed by red shift of 10 nm with further increase of acid concentration. The former was attributed to solvent dielectric effect and latter to the protonation of >C=O oxygen atom. Although in our case a continuous increase of absorbance was observed without any change in 328 nm absorption band maximum in 0.5–10 M acid concentration and slight blue shift in λ_{max}^{ab} in 10–18 M acid concentration, the results can be explained on the same lines. Hardly any change in λ_{max}^{ab} and slight blue shift in λ_{max}^{f} from $H_0 = 0$ to $H_0 = -5$ can be explained as follows. In case of 2-ABA or 2-DMABA the IHB is between amino lone pair and –COOH proton and >C=O is free for protonation. Whereas in our case IHB is between $-NH_2$ proton and >C=O oxygen atom. Protonation of >C=O group will lead to the breaking of cyclic structure of 2-ANA. This will lead to blue shift, whereas the protonation of >C=O group will lead to red shift. Thus the net effect may be zero or negligible on the spectral properties. A large red shift in λ_{max}^{f} with increase of acid concentration in the range of 10–18 M H_2SO_4 and appearance of isoemissive point observed in the acid concentration range of $H_0 = -5$ to $H_0 = -10$ suggests the formation of DC1. Single exponential observed in the fluorescence decay profile of species at $H_0 = -10$ (τ = 7 ns) suggests the presence of a single species. Although we are not able to measure the pK_a value for DC–MC equilibrium, fluorimetric titration method has given the pK_a^* as -7.9. Thus the minimum value of pK_a would be -7.9. These

values agree nicely with those observed for 2-DMABA [12]. Trication, obtained by further protonating $-NH_2$ of DC1 is not formed as one would require stronger acidic conditions than $H_0 = -10$.

5.4. Neutral-monoanion equilibrium

MA can only be formed by deprotonation of $-NH_2$ group. In 2-AP [1] pK_a for deprotonation is >16 and in 2-MAN its value is 11. Large decrease in the pK_a value for the deprotonation of $-NH_2$ is due to the presence of two electrons withdrawing groups present *ortho* to $-NH_2$ group and thus will decrease the charge density on the amino nitrogen atom. In general, MA formed by the deprotonation of $-NH_2$ group is non-fluorescent [15–22] with few exceptions [19]. Low Φ_f for the MA of aromatic amines in aqueous medium has been attributed to the solvent induced fluorescence quenching, because many of the MAs of aromatic amines becomes fluorescent in basic micellar medium [55]. A small decease in pK_a^* value suggests that $-NH_2$ group becomes stronger acid on excitation to S_1 state, consistent with literature data [14–20].

6. Conclusions

Above study has shown that: (i) 2-MAN is present as amine form rather than the imine one, (ii) ESIPT is not possible in 2-MAN, as only one normal Stokes shifted fluorescence band is observed. This process is endothermic in both S_0 and S_1 states involving high activation barrier energies, (iii) Only one monocation (MC1), one dication (DC1) and one MA are formed under different acid–base conditions. These are supported by different theoretical calculations.

Acknowledgements

The authors are thankful to the Department of Science and Technology, New Delhi for the financial support to the project number SP/S1/H-07/2000.

References

[1] A. Weisstuch, A.C. Testa, J. Phys. Chem. 72 (1968) 1982 (earlier references listed therein) ;
A.C. Testa, U.P. Wild, J. Phys. Chem. 85 (1981) 2637.
[2] S.G. Schulman, A.C. Capomacchia, M.S. Rietta, Anal. Chim. Acta 56 (1971) 91.
[3] J. Hager, S.C. Wallace, J. Phys. Chem. 89 (1985) 2637.
[4] B. Kim, C.P. Schick, P.M. Weber, J. Chem. Phys. 103 (1995) 6903.
[5] K. Inuzuka, A. Fujimoto, Spectrochim. Acta 42A (1986) 623.
[6] F. Hung, W. Hu, T. Li, C. Cheng, P.T. Chou, J. Phys. Chem. A 107 (2003) 3244.
[7] J. Konijnenberg, A.H. Huizer, C.A.G.O. Varma, J. Chem. Soc. Trans. Faraday 2 (85) (1989) 1539.
[8] A. Fujimoto, K. Inzuka, Bull. Chem. Soc. Jpn. 64 (1991) 3758.
[9] H. Ishikawa, K. Iwata, H. Hamuguchi, J. Phys. Chem. A 106 (2002) 2305.
[10] N. Mataga, Bull. Chem. Soc. Jpn. 36 (1963) 654.
[11] A. Tramer, J. Mol. Struc. 4 (1969) 313.
[12] A. Tramer, J. Phys. Chem. 74 (1970) 887.
[13] D.V.S. Jain, F.S. Nandel, P. Singla, D.J. Kaur, Indian J. Chem. 25A (1986) 15.
[14] J.F. Ireland, P.A.H. Wyatt, Adv. Phys. Org. Chem. 12 (1976) 132.
[15] M. Swaminathan, S.K. Dogra, Can. J. Chem. 61 (1883) 1064.
[16] A.K. Mishra, S.K. Dogra, J. Photochem. 105 (1983) 163.
[17] M. Swaminathan, S.K. Dogra, J. Am. Chem. Soc. 105 (1983) 6223.
[18] R.V. Subbarao, M. Krishnamurthy, S.K. Dogra, J. Photochem. 34 (1986) 55.
[19] A.K. Mishra, M. Swaminathan, S.K. Dogra, J. Photochem. 29 (1985) 87.
[20] R.V. Subbarao, M. Krishnamurthy, S.K. Dogra, Indian J. Chem. 25A (1986) 517.
[21] B.S. Furniss, A.S. Hunafols, V. Rogers, P.W.G. Smith, A.R. Talchall, Vogel's Text Book of Practical Organic Chemistry, ELBS, London, 1980.
[22] G. Krishnamoorthy, S.K. Dogra, J. Org. Chem. 64 (1999) 6566.
[23] M.M. Balamurali, S.K. Dogra, J. Photochem. Photobiol. A: Chem. 254 (2002) 181.
[24] M.J. Jorgenson, D.R. Hartter, J. Am. Chem. Soc. 79 (1957) 427.
[25] G. Yagil, J. Phys. Chem. 71 (1967) 1034.
[26] S.R. Meach, D.J. Phillips, J. Photochem. 23 (1983) 193.
[27] M.J.S. Dewar, E.G. Zoeblish, E.F. Healy, J.J.P. Stewart, J. Am. Chem. Soc. 107 (1985) 3092.
[28] Th. Arthen-Engeland, T. Bultmann, N.P. Ernsting, M.A. Roderiguez, W. Theil, Chem. Phys. 163 (1992) 43.
[29] J. Catalan, F. Fabero, M.S. Guijarro, R.M. Claramunt, M.D. Santa Marria, M.D.C. Foces-Foces, F.H. Cano, J. Elguero, R. Sastre, J. Am. Chem. Soc. 112 (1990) 746.
[30] B. Dick, J. Phys. Chem. 94 (1990) 5742.
[31] S. Santra, S.K. Dogra, Chem. Phys. 226 (1998) 285.
[32] J. Del Bene, H.H. Jaffe, J. Chem. Phys. 48 (1962) 1807.
[33] A. Kumar, P.C. Mishra, QCPE Bull. 9 (1989) 67.
[34] N. Mataga, T. Kubota, Molecular Interactions and Electronic Spectra, Marcel Dekker, New York, 1970.
[35] E. Lippert, Z. Electrochem. 61 (1957) 962.
[36] M. Head-Gordon, E.S. Replogle, J.A. Pople, Gaussian 98, A.T. Gaussian Inc., Pittsburg, PA, 1998 (revision).
[37] A.D. Becke, J. Chem. Phys. 98 (1993) 5648.
[38] R.G. Parr, W. Yang, Density Functional Theory of Atoms and Molecules, A.T. Gaussian Inc, Pittsburg, PA, 1998.
[39] G.A. Petersson, M.A. Al-Laham, J. Chem. Phys. 94 (1991) 6081.
[40] J.B. Foresman, A. Frisch, Exploring Chemistry with Electronic Structure Methods, second ed., Gaussian Inc, Pittsburg. PA, 1996.
[41] J.B. Foresman, M. Head-Gordon, J.A. Pople, M.J. Frisch, J. Phys. Chem. 96 (1992) 135.
[42] M.E. Casida, C. Jamorski, K.C. Casida, D.R. Salahub, J. Chem. Phys. 108 (1998) 439.
[43] R.F. Evans, E.F.G. Herington, W. Kynaston, Trans. Faraday Soc. 49 (1953) 1284;
R.W. Green, H.K. Tong, J. Am. Chem. Soc. 78 (1956) 4896.
[44] M.K. Nayak, S.K. Dogra, J. Mol. Struct. 202 (2004) 85.
[45] S. Srivastava, S.K. Dogra, J. Photochem. Photobiol. A: Chem. 46 (1989) 329.
[46] A. Kawski, F. Rabek (Eds.), Progress in Photochemistry and Photophysics, 5, CRC Press, Boca Ration, Fl., 1992, p. 2 (references listed therein).
[47] E. Lippert, Z. Naturforsch. 10A (1955) 541;
E. Lippert, Z. Naturforsch. 17A (1955) 590.
[48] N. Mataga, Y. Kaifu, M. Koizumi, Bull. Chem. Soc. Jpn. 28 (1955) 690.
[49] S. Mazumdar, R. Manoharan, S.K. Dogra, J. Photochem. Photobiol. A: Chem. 46 (1989) 301.

[50] M.B. Ledger, P. Suppan, Spectrochim. Acta 23A (1967) 3007.
[51] L. Goodman, H. Shull, J. Chem. Phys. 27 (1957) 1338; N. Mataga, Bull. Chem. Soc. Jpn. 36 (1963) 654.
[52] M.K. Nayak, S.K. Dogra, J. Photochem. Photobiol. A: Chem., in press.
[53] H.H. Jaffe, M. Orchin, Theory and Applications of Ultraviolet Spectroscopy, John Wiley, London, 1962.
[54] R.S. Moog, N.A. Burozski, M.M. Desai, W.R. Good, C.D. Silvers, P.A. Thompson, J.D. Simon, J. Phys. Chem. 95 (1991) 8466.
[55] R.S. Sarpal, S.K. Dogra, J. Chem. Soc. Faraday Trans. I 88 (1992) 2725.